J Mater Sci (2008) 43:6005–6011
DOI 10.1007/s10853-008-2640-z

Effect of finishing rolling temperature on fire resistance and dynamic strain aging behavior of a structural steel

Welbert Ribeiro Calado · Odair José dos Santos · Cynthia Serra Batista Castro · Ronaldo Neves Barbosa · Berenice Mendonça Gonzalez

Received: 14 December 2007 / Accepted: 8 April 2008 / Published online: 13 August 2008

Abstract The influence of finishing rolling temperature (FRT) on dynamic strain aging (DSA) behavior and high-temperature resistance of a fire resistant steel microalloyed with Mo and Nb was investigated by means of tensile tests performed at temperatures ranging from 25 to 600 °C and strain rates of 10^{-4} to 10^{-1} s^{-1}. In these steels, DSA manifestations are less intense than those observed for carbon steels and they take place at higher temperatures. The precipitation behavior of the steels was also considered. Hardness of samples heat treated at 100–600 °C displayed a maximum at 400 °C. Samples treated at this temperature and tensile tested at 600 °C did not show a higher yield stress than the untreated specimens. Results obtained indicated that DSA in the fire resistant steel might have a contribution for its fire resistance. The empirical activation energies related to the appearance of serrations on the stress–strain curves and to the maxima on the variation of tensile strength with temperature suggested that the high-temperature strengthening associated with DSA in this steel is the dynamic interaction of interstitial-substitutional solute dipoles and dislocations. The steel with lower FRT is more susceptible to DSA because of its higher amount of carbon in solid solution and showed better results in terms of high-temperature resistance.

W. R. Calado · R. N. Barbosa · B. M. Gonzalez (✉)
Department of Metallurgical and Materials Engineering, Universidade Federal de Minas Gerais, Rua Espirito Santo, 35, 30160-030 Belo Horizonte, MG, Brazil
e-mail: gonzalez@demet.ufmg.br

O. J. dos Santos
Usiminas, Research and Development Center, Av. Pedro Linhares Gomes, 5431, 35160-900 Ipatinga, Brazil

C. S. B. Castro
Metallurgical Technology Division, Fundação Centro Tecnológico de Minas Gerais, Av. José Cândido da Silveira, 2000, 30170-000 Belo Horizonte, MG, Brazil

Introduction

Structures using conventional structural steel require fire resistant coating or insulation to achieve the desired fire resistance in fire sensitive areas, which can cost around 50% of the steel pride and its application can extend the construction period of the building by several weeks, thus creating another cost penalty [1]. The problem with unprotected carbon-manganese steel is its poor strength at temperatures above ~350 °C, which can make a structure unsafe after a major fire, difficult to assess the damage caused by a short duration fire and may call for demolition or renovation of the structures. A fire resistant steel, which requires little or no fire protection, could lead to cheaper and faster construction and advantages in other ways, such realization of economical structure design, unnecessary measures to prevent falling off from protected steel and maximum use of space [2]. Fire resistant steels must have their yield strength at 600 °C as 67% of the specified value at room temperature [3]. Previous studies on microstructure and mechanical proprieties of fire resistant steels carried out by Kamada et al. [4] and Chijiiwa et al. [3] focused on processing, structure and properties of fire resistant steel with different combinations of alloying elements. They are low carbon steels which generally have Mn, Mo, Cr, and Nb, Ti or V in their composition. In steels alloyed with Mo, Mn, and Cr or microalloyed with Nb, Ti, and V the high-temperature strength related to dynamic strain aging (DSA) has been attributed to the phenomenon known as interaction solid-solution hardening, ISSH, due to the dynamic

interaction of interstitial-substitutional pairs and dislocations. The ISSH effect displaces DSA manifestations to higher temperatures than those displayed by mild carbon steels so is an important contribution to the creep resistance of these steels [5–7]. Solid solution and precipitation hardening have been considered, among other mechanisms, as important effects responsible for higher temperature resistance in fire resistant steel [8–10]. The influence of DSA on creep resistance of steels suggests that this process would enhance the high-temperature strength of fire resistant steels. The present work was undertaken to characterize the effect of the finishing rolling temperature (FRT) on the DSA susceptibility and identify its influence on the fire resistance of a Mo-Nb structural steel.

Experimental

The fire resistant steels studied, whose chemical composition (in weight percent) is showed in Table 1, were received in hot rolled condition as 12.7 mm in thickness plate. The steels were manufactured with controlled rolling and finishing at temperatures of 800 and 850 °C.

The microstructure characterization of steel was performed in the transverse section prepared by standard metallographic techniques. Specimens observed by optical and scanning electron microscopy (SEM) were chemically etched with 4% nital. Images were examined for determination of the volume fraction of phases and measurement of ferrite grain size. The 2.5 mm diameter and 27.0 mm gauge length tensile test specimens were machined along the rolling direction.

The tensile tests were performed in a servo hydraulic MTS testing machine in a temperature range from 25 to 600 °C, at strain rates of 10^{-4}, 3.5×10^{-3}, 10^{-3}, 10^{-2} and 10^{-1} s^{-1}. Before testing, samples were held for 5 min at the test temperature. The heating system used kept temperature stable with maximum variations less than ±2 °C and with a negligible temperature gradient along the length of the sample. The values of yield strength, σ_y, ultimate tensile strength, σ_t, and total elongation, e_t, were determined as the average of at least three tensile tests performed at identical conditions. The relative error in the values of stress and elongation was lower than 3%.

The Vickers hardness measurements, using a load of 30 kgf, were made on transverse section of the plates heat treated from 100 to 400 °C for 30 min.

Table 1 Chemical composition of steels (% weight)

C	Mn	Mo	Cr	Si	P	S	Nb	Al	N
0.092	0.80	0.19	0.10	1.21	0.038	0.0045	0.020	0.018	0.0052

The amount of nitrogen and carbon in solid solution was calculated using the software Thermo-Calc for Windows, database TCFES: TCS Steels/Fe-alloys, v5.

Results and discussion

The microstructure of the steel consisted of ferrite, pearlite, and martensite. The volume fractions and ferrite grain sizes are presented in Table 2. The FRT800 and FRT850 steels have practically the same amount of phases, however the ferrite grain size showed a small difference between the steels. The grain size of first steel is smaller, with a difference less than 2 μm, than of the second.

Stress–strain curves for the FRT800 and FRT850 steel tested at various temperatures and at a strain rate of 10^{-4} s^{-1} are shown in Fig. 1a and Fig. 1b, respectively. The Portevin-LeChatelier Effect (PLC) was present at a certain temperature interval and the same was observed for tests performed at the four other strain rates. The temperature at the onset of the serrations was observed to increase for increasing strain rates. Figure 1 shows also that the work hardening rate increases with temperature between 150 and 300 °C for the FRT800 and FRT850 steels.

For the five rates employed and the two steels studied, the value of the yield stress, σ_y, at 600 °C was higher than 67% of its minimum specified value at room temperature for this class of structural steel, 325 MPa. The changes in yield stress, σ_y, and tensile strength, σ_t, with temperature are shown in Fig. 2a and Fig. 2b for FRT800 and FRT850 steels, respectively, for the five strain rates considered. It can be observed that, the fire resistants steels show maxima in σ_t occurring at increasing temperatures for increasing strain rates (Table 3). The amplitude of these maxima decreases as the strain rate is increased. The σ_y curves display plateaux in the temperature interval at which the maxima in σ_t were observed for the five strain rates considered and for the two steels studies.

Figure 3a and b shows the changes in the total elongation, e_t, with test temperatures for the five strain rates investigated for the FRT800 and FRT850 steels, respectively.

These figures show that e_t decreased with increases in temperature, presenting a minimum at a certain temperature and then it increased with raising temperatures. For a strain rate of 10^{-3} s^{-1} this minimum appear at a

Table 2 Volume fractions of ferrite, pearlite, martensite, and ferrite grain size (GS)

Steel	Pearlite (%)	Martensite (%)	Ferrite (%)	GS (mm)
FRT800	9.7 ± 0.9	2.7 ± 0.4	Balance	6.7 ± 0.3
FRT850	9.7 ± 0.8	2.8 ± 0.7	Balance	9.1 ± 0.3

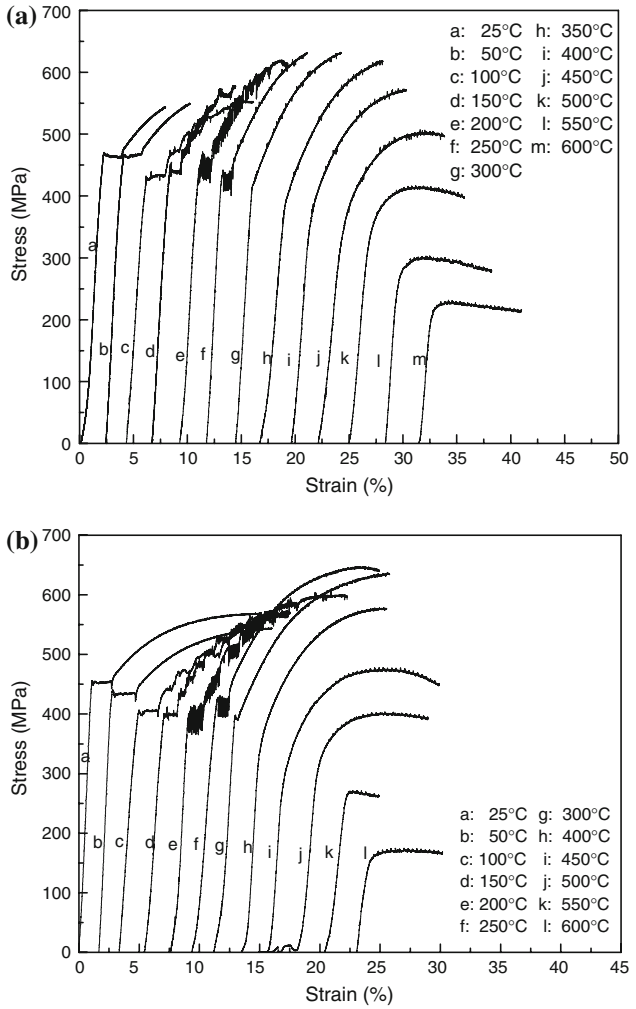

Fig. 1 Stress–strain curves for specimens tested at a strain rate of 10^{-4} s^{-1} at various temperatures. (**a**) FRT800 steel, (**b**) FRT850 steel

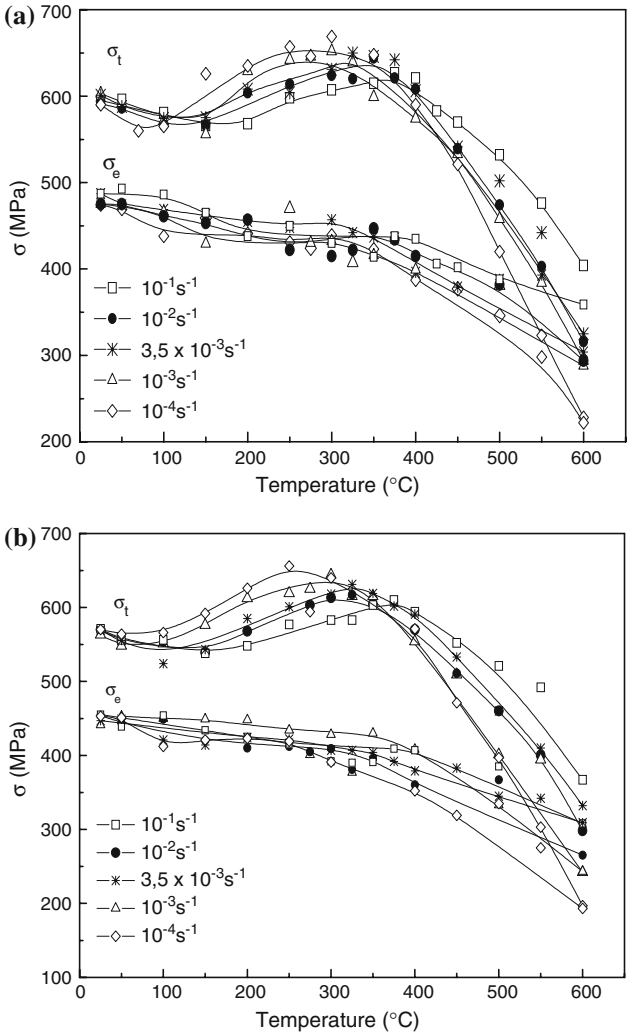

Fig. 2 Changes in yield stress and tensile strength with temperature for the fire resistant steel investigated at the five strain rates employed. (**a**) FRT800 steel, (**b**) FRT850 steel

temperature of 215 and 245 °C for FRT800 and FRT850 steel, respectively; increasing strain this temperature increasing, for example, in a strain rate of 10^{-1} s^{-1} it change for 275 and 320 °C, respectively. The existing of a high-temperature minimum in ductility in addition to the one associated with the normal 'blue brittleness' effect follows a similar pattern to the variation of elongation to fracture observed by Baird and Jamison in steel containing Mo and Cr. This has been ascribed to localized work softening due to exhaustion of the solute atoms required to pin dislocations by DSA and the same explanation could hold at low temperatures [6].

Figure 4a compare the yield stress and tensile strength for both steels for a strain rate of 10^{-2} s^{-1}. The FRT800 steel presents mechanical properties and fire resistance better than FRT850 steel, probably due the higher amount of carbon retained in solid solution, according to the results obtained by using the Thermocalc software, 113 and 86 ppm, respectively. The total elongation behaviors of the two steels are similar and their minima for the FRT800 steel appear at a temperature lower than that in FRT850 (Fig. 4b).

Table 3 Temperature at the conditions concerning the onset of the PLC effect and the maximum in tensile strength

Steel	Onset of the PLC		Maximum in tensile strength	
	$\dot{\varepsilon}$ (s^{-1})	Temperature (°C)	$\dot{\varepsilon}$ (s^{-1})	Temperature (°C)
FRT800	10^{-1}	175	10^{-1}	375
	10^{-2}	145	10^{-2}	350
	10^{-3}	109	10^{-3}	300
	10^{-4}	80	10^{-4}	275
FRT850	10^{-1}	185	10^{-1}	375
	10^{-2}	140	10^{-2}	325
	10^{-3}	107	10^{-3}	300
	10^{-4}	85	10^{-4}	275

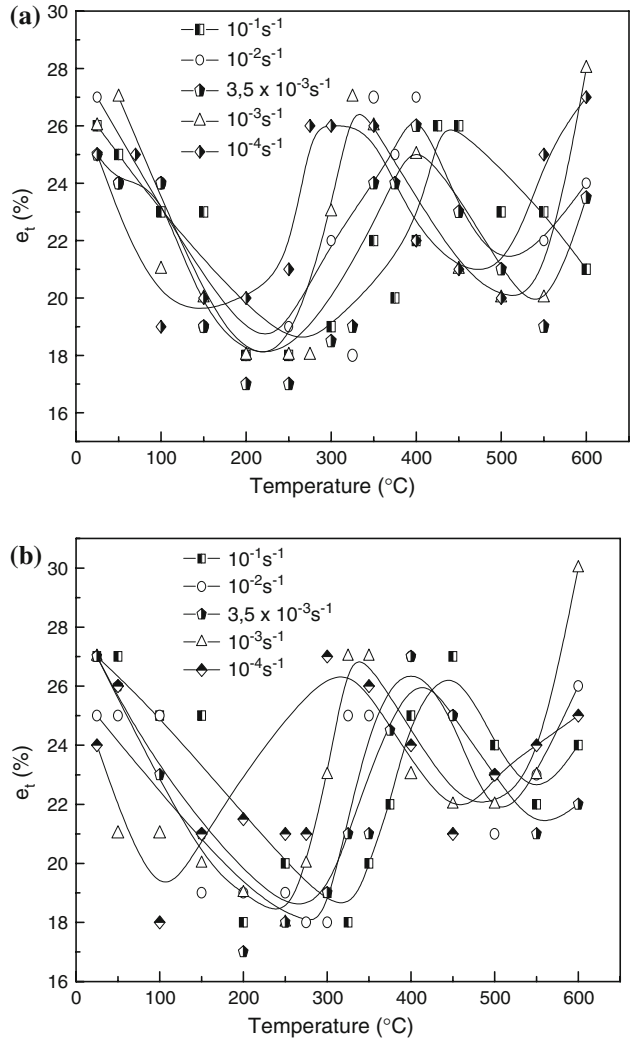

Fig. 3 Changes in elongation with temperature for the fire resistant steel investigated at the five strain rates employed. (**a**) FRT800 steel, (**b**) FRT850 steel

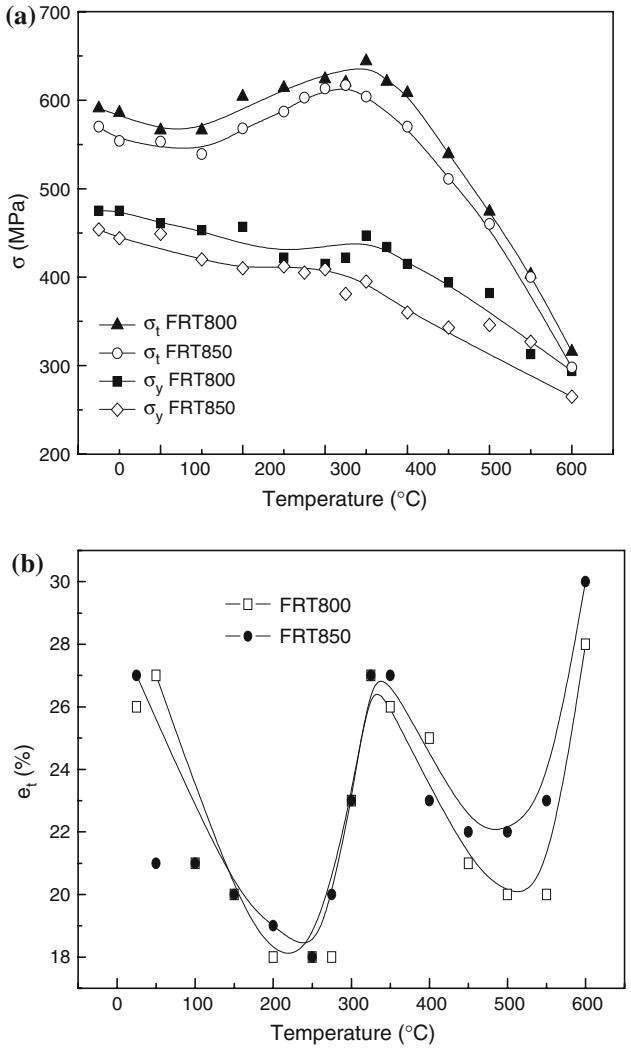

Fig. 4 Temperature variations of (**a**) Yield stress and tensile strength at strain rate of 10^{-2} s^{-1} and (**b**) Total elongation at strain rate of 10^{-3} s^{-1}

The characteristics of Portevin-LeChatelier (PLC) effect in terms of strength maximum, elongation minimum, athermal yield stress (plateaux in the yield stress versus temperature) along with increasing word hardening rates with increasing temperature are similar to those found in low carbon steels, however, these manifestations take place at higher temperatures. For a given strain rate the strength of the maximum in σ_t can be defined as the difference between this maximum (σ_{tmax}) and the minimum value of σ_t (σ_{tmin}) between room temperature and the temperature of σ_{tmax}. For a strain rate of 10^{-2} s^{-1}, the temperature at which the maximum in σ_t occurs in the FRT800 steel is about 350 °C, and the value of σ_{tmax}–σ_{tmin} is approximately 80 MPa. For the FRT850 the temperature of the maximum is about 325 °C, and the value of σ_{tmax}–σ_{tmin} is approximately 64 MPa. According to the analyses with Thermocalc the amount of soluble nitrogen in the FRT800 and FRT850 in their FRT are 0.1 and 0.3 ppm, respectively; these are considered very small values. So the effects of DSA might be attributed to the carbon retained in solid solution on FRT, namely 113 and 86 ppm for the FRT800 and FRT850 steel respectively. This displacement to higher temperatures of DSA manifestations in steels microalloyed with niobium and or vanadium was already reported [7, 11].

According to the literature [12, 13], the minimum absolute temperature, T, associated with the occurrence of the PLC effect in low carbon steels is related to the strain rate, $\dot{\varepsilon}$, by the equation:

$$\dot{\varepsilon} = \frac{B\rho_m bl}{T}\exp\left(-\frac{Q}{RT}\right) \quad (1)$$

where B is a constant, ρ_m is the density of mobile dislocations, l is the average distance traveled by dislocations

between penetable obstacles, b is the Burgers vector, R is the universal gas constant, and Q is the activation energy of the process. Assuming that the term $B\rho_m bl$ remains constant when T and $\dot{\varepsilon}$ vary, the value of the apparent activation energy, Q, can be determined from a $\ln(\dot{\varepsilon} \cdot T)$ versus T^{-1} plot. The values usually found for this apparent activation energy are of the order of the activation energies for diffusion of N and C atoms responsible for dislocation locking [12–14]. The absolute temperature at which the PLC effect ends, which coincides with the temperature corresponding to the maximum in σ_t [12], is also related to the strain rate by an expression similar to Eq. 1. The values of Q found in this case have been associated with the sum of the activation energy for diffusion of the solute responsible for dislocation locking and the solute-dislocation binding energy. This association is based on the hypothesis that, at this stage, solute atoms are dragged by dislocations during their movement [12].

The values reported for the activation energy for the start of serrated flow in low carbon steels range from 79.5 kJ/mol to 84.1 kJ/mol [12, 13] and are close to the activation energies for diffusion of N and C in ferrite, respectively, 76.1 kJ/mol and 84.1 kJ/mol [15]. Typical values of the activation energy associated with the disappearance of serrated flow, Q′, are 127.6 kJ/mol [12] and 134 kJ/mol [13], while those related to the maximum in tensile strength are 127.6 kJ/mol to 156.1 kJ/mol [12, 14]. The lower values for the activation energies related to the end of the PLC effect and to the presence of the maximum in σ_t have been attributed to dislocation locking by nitrogen atoms, while the higher values have been associated to dislocation locking due to carbon atoms. Intermediate values found for these energies reflect the combined effect of C and N. Thus, considering the minimum values of these activation energies, the binding energy of N atoms to dislocations in ferrite can be estimated, while the carbon-dislocation binding energy is estimated using the maximum value of these activation energies. In the case of N, the binding energy should be 127.6 kJ/mol–79.5 kJ/mol, equal to 48.1 kJ/mol (0.50 eV). For C atoms, the value is 156.1 kJ/mol–84.1 kJ/mol, or 72.0 kJ/mol (0.75 eV). These values are in good agreement with the classical solute-dislocation binding energies in ferrite for N atoms, 0.47 eV [16], and for C atoms, 0.75 eV [17].

In this study, the serrated flow, the maximum in σ_t and the minimum in e_t indicate that DSA was taking place. Thus, apparent activation energies can be estimated for these processes, as described before. Figure 5 shows $\ln(\dot{\varepsilon} \cdot T)$ versus T^{-1} for the onset of the PLC effect, the end of serrated flow and the values obtained from the slopes of these plots, which are, respectively, 97±4 kJ/mol (Q), and

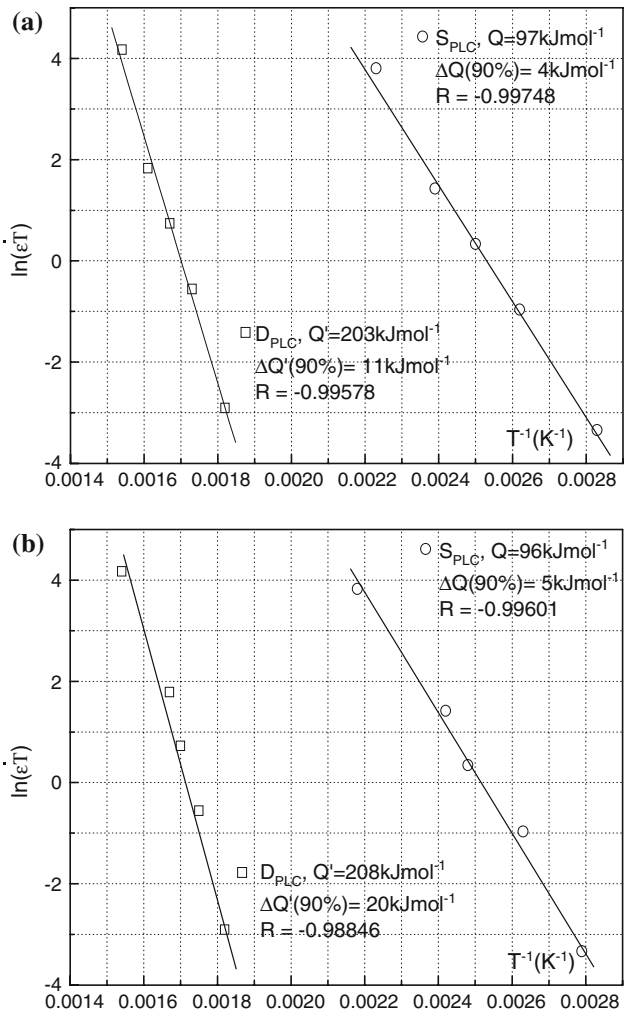

Fig. 5 $\ln(\dot{\varepsilon} \cdot T)$ versus T^{-1} at the conditions concerning the onset of the PLC effect and the maximum in tensile strength, σ_t. (**a**) FRT800 steel, (**b**) FRT850 steel

203±11 kJ/mol (Q′) for the FRT800 steel, and 96±5 kJ/mol (Q), and 208±20 kJ/mol (Q′) for the FRT850 steel. The first of these values in both steels is considerably higher than the activation energies associated with dislocation locking by N and C atoms in solid solution in ferrite, namely 79.5 kJ/mol to 84.1 kJ/mol. The value for the end of serrated flow is higher than the activation energies found in low carbon steels for the end of the PLC effect and the occurrence of the maximum in σ_t (127.6–151.6 kJ/mol) for the two steels. These results suggest that the DSA effects found in the fire resistant steel should be controlled by a mechanism in some aspects different from that operating in carbon steels.

As already mentioned, in steels containing Mn, Mo, Cr, Ti, and Nb, interstitial N and C are in close association with substitutional forming interstitial-substitutional dipoles that interact strongly with dislocations over a large temperature

range, the effect of interaction solid-solution hardening, ISSH [5, 6] If the interaction energy between interstitials and dislocations is higher than the interaction energy between interstitials and substitutionals the extra high-temperature strengthening will be due to a displacement of the DSA effects associated with N and C to higher temperatures due to a reduction in the mobility of dislocation atmospheres [6]. As the fire resistant steels displayed DSA manifestations, it seems that the ISSH effect on DSA is a contribution to the fire resistance in addition to precipitation hardening and solid-solution hardening.

The difference in the values of activation energies for the onset of the PLC effect and for the occurrence of the maxima in σ_t, 106 kJ/mol (1.1 eV) for FRT800 steel and 112 kJ/mol (1,2 eV) for the FRT850 steel are higher than the values of the N-dislocation and C-dislocation interaction energies, 0.47 and 0.75 eV, respectively [16, 17], indicating that DSA in this steel is related to locking of dislocations by atmospheres of N and C atoms whose mobility is reduced due to the interstitial-substitutional interaction as discussed for the effect of Mn on the strain aging due to N and C in a Nb microalloyed steel [7].

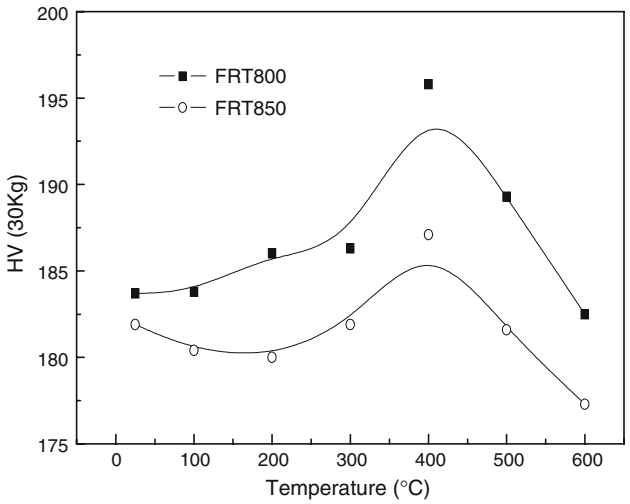

Fig. 6 Variation in hardness with temperature of samples submitted to a 30 min heat treatment

Figure 6 shows the changes in hardness with temperature for heat treated samples for the two steels studied. The maximum in hardness observed at 400 °C is probably associated with secondary precipitation of Mo carbides. According to Lenk et al. [18], the precipitation of Mo_2C is a significant contribution to high-temperature resistance in steels. The FRT800 steel has higher hardness due to its larger amount of carbon atoms in solid solution.

The analysis of Table 4 indicates that secondary precipitation has a small effect on the yield stress at 25 °C in the considered steels. On the other hand, this effect has no influence on the yield stress at 600 °C. At such high temperatures the carbides precipitated at 400 °C are not effective in keeping resistance because of Ostwald Ripening.

Conclusions

1. The fire resistant steel considered in this work presents DSA phenomena similar to those displayed for low carbon steels. However, DSA take place at higher temperatures.
2. The values of the apparent activation energy related to the onset of the PLC effect and to the maximum in ultimate tensile strength versus temperature curves, indicate that, in this fire resistants steels, the mobility of dislocation atmospheres, which controls DSA, is affected by substitutional solutes such as Mn, Cr, Mo, and Nb.
3. The ISSH effect present in the steel studied here adds up to a contribution to fire resistance properties of the steel through the DSA phenomenon much in the same way that it contributes to creep resistance of heat resistant steels.
4. The FRT influences the fire resistance. In the lower temperature (800 °C) the quantity of carbon retained in solid solution is higher than that in the high temperature (850 °C). The FRT800 steel is more susceptive to DSA phenomenon and more fire resistant.
5. Secondary precipitation in the fire resistant steels studied does not contribute to their fire resistance.

Table 4 Yield stress and tensile strengths for FRT800 and FRT850 steels untreated and 400 °C treated for 30 min

Steel	Test temperature (°C)	σ_y (MPa)	σ_t (MPa)	$\sigma_{y\ (treated)}$ (MPa)	$\sigma_{t\ (treated)}$ (MPa)
FRT800	25	475 ± 2	603 ± 4	492 ± 10	609 ± 9
	600	288 ± 2	294 ± 4	289 ± 4	288 ± 10
FRT850	25	441 ± 6	563 ± 1	458 ± 5	576 ± 6
	600	236 ± 4	243 ± 9	239 ± 11	257 ± 1

References

1. Kelly FS, Sha W (1999) J Construct Steel Res 50:223. doi: 10.1016/S0143-974X(98)00252-1
2. Keira K (1998) Nippon Steel Tech Rep 77:88
3. Chijiiwa R, Yoshida Y, Uemori R, Tamehiro H, Funato K, Horii Y (1993) Nippon Steel Tech Rep 58:47
4. Kamada Y, Fukuda Y, Nakazato T, Hirayama H, Kawano K, Ogata R (1991) Sumitomo Met Tech Rep 47:23
5. Leslie WC (1982) The physical metallurgy of steels. McGraw-Hill Book Company, New York
6. Baird JD, Jamielson A (1972) JISI 210:841
7. Gunduz S (2002) Ironmak Steelmak 29:341. doi:10.1179/030192302225004575
8. Sha W, Kelly FS, Browne P, Blackmore SPO (2002) J Mater Eng Perform 8:606. doi:10.1007/s11665-999-0017-3
9. Sha W (2004) Mater Sci Technol 20:449. doi:10.1179/026708304225012305
10. Panigrahi BK (2006) Bull Mater Sci 29:59
11. Karabuk H, Gunduz S (2004) Mater Sci Des 25:521. doi: 10.1016/j.matdes.2004.01.005
12. Keh AS, Nakada YW, Leslie WC (1968) In: Rosenfield AR, Hahn GT, Bement AL Jr, Jaffee RI (eds) Dislocation dynamics, McGraw Hill, New York, p 81
13. Taheri AK, Maccagno TM, Jonas JJ (1995) ISIJ Inter 35:1532. doi:10.2355/isijinternational.35.1532
14. Espíndola M, Weidig C, Rodrigues PCM, Andrade MS, Gonzalez BM (1995) Wire J Int 28:85
15. Porter DA, Easterling KE (1996) Phase transformation in metals and alloys. Chapman & Hall, London
16. Petarra DP, Beshers DN (1965) Acta Metall 15:791. doi: 10.1016/0001-6160(67)90360-4
17. Cochardt AW, Schoek G, Wiedersich H (1955) Acta Metall 3:533. doi:10.1016/0001-6160(55)90111-5
18. Lenk P, Melser B (1994) Int J Pres Ves Pip 58:361. doi: 10.1016/0308-0161(94)90073-6